Solvation of Magnesium Dication: Molecular Dynamics Simulation and Vibrational Spectroscopic Study of Magnesium Chloride in Aqueous Solutions

Karen M. Callahan,[†] Nadia N. Casillas-Ituarte,[‡] Martina Roeselová,[§] Heather C. Allen,[‡] and Douglas J. Tobias*,[†]

Environmental Molecular Science Institute and Department of Chemistry, University of California, Irvine, California 92697, Department of Chemistry, The Ohio State University, 100 West 18th Avenue, Columbus, Ohio 43210, Center for Biomolecules and Complex Molecular Systems, Institute of Organic Chemistry and Biochemistry, Academy of Sciences of the Czech Republic, Flemingovo námisti 2, 16610 Prague 6, Czech Republic

Received: September 22, 2009; Revised Manuscript Received: January 26, 2010

Magnesium dication plays many significant roles in biochemistry. While it is available to the environment from both ocean waters and mineral salts on land, its roles in environmental and atmospheric chemistry are still relatively unknown. Several pieces of experimental evidence suggest that contact ion pairing may not exist at ambient conditions in solutions of magnesium chloride up to saturation concentrations. This is not typical of most ions. There has been disagreement in the molecular dynamics literature concerning the existence of ion pairing in magnesium chloride solutions. Using a force field developed during this study, we show that contact ion pairing is not energetically favorable. Additionally, we present a concentration-dependent Raman spectroscopic study of the $Mg-O_{water}$ hexaaquo stretch that clearly supports the absence of ion pairing in $MgCl_2$ solutions, although a transition occurring in the spectrum between $0.06x$ and $0.09x$ suggests a change in solution structure. Finally, we compare experimental and calculated observables to validate our force field as well as two other commonly used magnesium force fields, and in the process show that ion pairing of magnesium clearly is not observed at higher concentrations in aqueous solutions of magnesium chloride, independent of the choice of magnesium force field, although some force fields give better agreement to experimental results than others.

1. Introduction

Aqueous Mg^{2+} is important to a wide range of biological and inorganic systems. In several instances, magnesium is used to stabilize structures, such as cell membranes, proteins, DNA, and RNA.[1−4] Additionally, it plays a catalytic role in many enzymes, for example, enabling hydrolysis and condensation reactions that normally occur at extremes of pH to occur at biologically relevant pH values.[1] The involvement of Mg^{2+} in biological functions occurs not only through direct interactions with biological molecules, but also in interactions through the solvent shell of fully hydrated magnesium dications.[1−4]

The role of Mg^{2+} in environmental chemistry has been less well explored. Mg^{2+} is the second most common cation in seawater (after sodium),[5] making its effects on sea spray and aged sea salt aerosols an issue of atmospheric relevance. Due to the low relative humidity required for deliquescence of $MgCl_2$ relative to NaCl (33.0% rather than 75.5% at 20 °C),[6] laboratory experiments have employed Mg^{2+} in concentrations comparable to sea salt to provide a liquid layer on the surface of powdered NaCl.[7] At aqueous interfaces, chloride ions participate in heterogeneous reactions forming molecular chlorine, although the reaction does not occur on solid NaCl and is not atmospherically significant in bulk solutions of NaCl.[7−9]

Mg^{2+} may play an even larger role in inland aerosols formed when windblown dried playa sediments become cloud condensation nuclei. Owens Lake bed in California is one of the largest sources of dust aerosol in the Western Hemisphere.[10,11] Samples of the crust of the dry Owens Lake bed show greater concentrations of Mg^{2+} and Ca^{2+} relative to Na^+ than seen in seawater aerosols.[10] Mg^{2+} and Ca^{2+} are more hygroscopic than Na^+ and affect the water uptake and nucleation of mixed salt particles.[12,13]

Given the ubiquitous use of Mg^{2+} in biology for structural stabilization and catalysis and its presence in a wide range of environmental aerosols, we seek a fundamental understanding of the solvation structure of magnesium in aqueous solutions, which shall then be extended to its behavior at the interfaces.[14,15] This study focuses on magnesium chloride in bulk aqueous solution. Chloride was chosen as the anion because of its prevalence in atmospheric marine aerosols.

Molecular dynamics (MD) simulations of bulk aqueous $MgCl_2$ solutions have previously been performed at a variety of concentrations.[2,16−22] In addition to classical MD studies, there have been several first-principles MD and Monte Carlo calculations of the hydration of Mg^{2+} in small clusters.[23−28] First-principles calculations on small clusters of water with magnesium dication[17,29−38] and first-principles MD simulations have been utilized to study the solvation of magnesium in bulk simulations at infinite dilution.[23−26,39] Ab initio and density functional theory (DFT) calculations as well as Car−Parrinello molecular dynamics (CPMD) simulations show that the first solvation shell of magnesium coordinates six water molecules at a distance ranging from 2.01 Å to 2.13 Å.[17,29−37] Both theory and experiments also show that the water molecules in the first solvation shell around magnesium are arranged in a distinct octahedral geometry (Figure 1). It has been established by ab

* To whom correspondence should be addressed. E-mail: dtobias@uci.edu.
[†] University of California, Irvine.
[‡] The Ohio State University.
[§] Academy of Sciences of the Czech Republic.

10.1021/jp909132a
Published on Web 03/04/2010

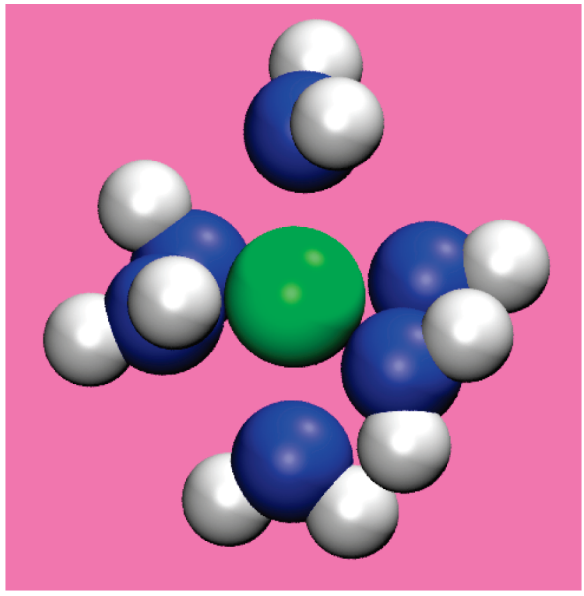

Figure 1. The first solvation shell of magnesium cation coordinates six water molecules at octahedral sites.

initio and DFT calculations as well as NMR, Raman spectroscopy, and X-ray absorption spectroscopy (XAS) experiments that magnesium interactions with water molecules in the first solvation shell are far stronger than most other cations.[23,25,36,40−42] Classical MD force fields tend to reproduce these properties.

In finite-concentration salt solutions, aggregation of cations and anions may occur. In this paper we will use the term contact ion pair when a cation and anion are adjacent to each other. Additionally, we will define a solvent-shared ion pair as a cation and anion separated by a water molecule that is in the first solvation shell of both ions, and a solvent separated ion pair a pair of ions that are separated by both of their first solvent shells. This is consistent with previous studies.[43,44] Previous MD simulations of aqueous $MgCl_2$ at low concentrations did not focus on the issue of ion pairing, owing to low numbers of cations and anions present in the simulated system. However, at higher concentrations it becomes more likely for ions to be near each other, increasing the probability of ion pairing if it is energetically favorable. Zapalowski et al. reported the presence of ion pairing in their classical MD simulations in the concentration range of 1.1−4.9 M $MgCl_2$, increasing with concentration.[22] However, the results of MD simulations are dependent on the force fields used to describe the interaction between the ions and molecules as well as the initial coordinates of the system. It is, therefore, beneficial to compare MD results to both first-principles calculations and experimental results.

Contrary to the results of Zapalowski et al., a DFT study of clusters of magnesium, chloride, and six water molecules by Waizumi et al. showed that chloride prefers to share water with solvated magnesium.[36] Waizumi et al. predicted that the magnesium holds the water molecules so tightly that the chloride is not able to dislodge them to form the contact ion pair, even though the binding energy between magnesium and chloride is much larger than that between magnesium and water.

The high energetic barrier to removing a water molecule from a magnesium dication presents an additional complication to showing whether there are ion pairs in equilibrium simulations. The lifetime of water in the first solvation shell of magnesium was observed by O^{17} NMR to be >1.8 μs in 0.063x $Mg(ClO_4)_2$.[45] This suggests that it would not be feasible to sufficiently sample possible solvation shells of magnesium in aqueous magnesium chloride solutions using MD if ion pairing was an important possibility. In fact, it has been observed in CPMD, quantum mechanics/molecular mechanics (QM/MM) and classical MD simulations that water molecules in the first solvation shell of a fully solvated magnesium do not exchange during the entire simulation (on time scales up to 5 ns), although Tongraar et al. observed occasional rearrangement within the first solvation shell.[23,25,26]

In this study, we use MD simulations in conjunction with Raman spectroscopy to investigate the solvation characteristics of aqueous Mg^{2+}. Validation of the standard Mg^{2+} force fields at high bulk concentration (0.0888x, where x is mole fraction, or 4.45 M, where M denotes molarity) in the presence of polarizable water and chloride is reported, and a new improved Mg^{2+} force field is developed. A comparison of MD simulation results to Raman spectroscopy, as well as to previously reported X-ray diffraction experiments, is then used to shed light on the issue of magnesium-chloride aggregation, and to establish the absence of ion pairing in $MgCl_2$ solution up to fairly high concentrations.

2. Methods

2.1. Computational Methods. Model solutions containing magnesium chloride were studied using classical MD simulations with three-dimensional periodic boundary conditions. Bulk simulations at "infinite dilution" contained 461 water molecules, one Mg^{2+}, and two Cl^- in a unit cell of 24 Å × 24 Å × 24 Å (this corresponds to 0.0022x, 0.12 M). The potentials of mean force (PMFs) for water and chloride approaching magnesium were computed using umbrella sampling to quantify the relative strengths of magnesium−water and magnesium−chloride interactions. Simulations for the PMF calculation were equilibrated for 100 ps each, and then 100 ps were used for data collection in each window. The umbrella sampling was performed using harmonic restraints to obtain overlapping distributions of the distance between magnesium and chloride or water from approximately 9 Å apart to approximately 2 Å apart in 0.2 Å increments. The harmonic biasing potential was 240 kcal/mol in the range (1.8 Å, 4.8 Å), and 120 to 240 kcal/mol in the range (5 Å, 9 Å). The program WHAM from the Grossfield laboratory was employed to unbias these distributions and obtain the PMF.[46]

Bulk simulations at 0.0888x (4.45 M, determined by the number of $MgCl_2$ and the volume of the unit cell), containing 780 water molecules and 76 $MgCl_2$, were equilibrated for at least 400 ps followed by at least 400 ps of data collection. The unit cell dimensions in these simulations were approximately 30 Å × 30 Å × 30 Å. Two sets of these simulations were performed. One set of initial coordinates was prepared with ∼90% of Mg^{2+} involved in contact ion pairs. The other set contained no contact ion pairs in the initial conditions. The initial configuration in this case was obtained by first preparing small clusters, each containing a hexa-hydrated magnesium, two chloride ions, and additional water molecules cut out from the simulation at "infinite dilution". Upon a brief equilibration, the clusters were placed on a grid, and then allowed to spontaneously condense into a bulk system.

The force field parameters used are listed in Table 1. ff99[47] is a force field developed for the AMBER package[48] based on calculations by Åqvist.[49] OPLSAA[50] is a force field developed by Jorgensen. A new Mg^{2+} parameter set was developed for the purpose of this study by fitting the Lennard-Jones parameters to reproduce the $Mg^{2+}-O_{water}$ distance calculated from X-ray diffraction studies of $MgCl_2$ solutions. We refer to this parameter set as "Callahan". All of the simulations incorporated the

TABLE 1: Simulation Parameters

atom	parameter set	q (e)[a]	α (Å^3)[b]	r (Å)[c]	ε (kcal/mol)[d]
Mg^{2+}	Åqvist/ff99[e]	+2	0.120	0.7926	0.8947
	OPLSAA[f]	+2	0.000	0.9929	0.8750
	Callahan	+2	0.000	1.0600	0.8750
Cl^-	PB[g]	−1	3.250	2.4192	0.1000
O	POL3[h]	−0.730	0.528	1.798	0.156
H	POL3[h]	0.365	0.170	0.0	0.0

[a] Charge of ion or partial charge of atom. [b] Polarizability. [c] Lennard-Jones radius. [d] Lennard-Jones well depth. [e] Cornell et al.,[47] Åqvist.[49] [f] Jorgensen.[50] [g] Perera and Berkowitz.[52] [h] Caldwell and Kollman.[51]

polarizable POL3 water model[51] and the chloride model of Perera and Berkowitz (PB).[52] The MD program employed was Sander in the AMBER 8 suite of programs[48] with a modified calculation of induced dipole to avoid polarization catastrophe, although we found this modification to be unnecessary in the absence of $Mg^{2+}-Cl^-$ ion pairing.[53] The smooth particle mesh Ewald sum was used to calculate electrostatic interactions.[54] The real space part of the Ewald sum and the Lennard-Jones interactions were truncated at 10 Å cutoff in the infinite dilution simulations and 12 Å for the other bulk simulations.[54,55] The time-step was 1 fs and trajectory data were recorded every picosecond. Water bond lengths and angles were constrained using the SHAKE algorithm.[56] All simulations were performed at constant temperature and pressure. The temperature was maintained with a Berendsen thermostat using a 1 ps time constant to an average temperature of 300 K.[57] The pressure was controlled to an average of 1 bar using an isotropic position scaling and a weak coupling scheme with a 1 ps relaxation time.[57] The VMD (Visual Molecular Dynamics) program was used to render the simulation snapshot in Figure 1.[58]

2.2. Experimental Methods. Raman spectra for Figure 3a,b were obtained using 150 mW from a 532-nm continuous wave laser (Spectra-Physics, Millennia II). The sample solution was contained in a 2 mL glass vial. The beam was focused ∼2 mm inside the vial using a 5 mm focusing Raman probe (InPhotonics). The Raman scatter was focused with a BK7 lens at the entrance slit of a 500 mm monochromator (Acton Research, SpectroPro SP-500). The residual 532 nm light was removed with a long-pass 535 nm filter (Omega Optical) before entering the monochromator. The Raman scatter was dispersed by a 1200 groove/mm grating blazed at 1 μm and collected on a liquid nitrogen-cooled CCD camera. The slit width was set to 100 μm. Calibration of the monochromator was completed by the procedure described elsewhere.[43] Raman spectra were acquired with 10 min of exposure time and at ∼22 °C. The average of two Raman spectra is shown. For Figure 3b, error bars show ± one standard deviation derived from the spectral fits (IgorPro 4.05). For Figure 3c, Raman spectra were obtained with a Raman Microscope (Renishaw inVia; Ohio State Department of Chemistry microscope facility) using 60 microwatts from a 785-nm continuous wave laser and a 1200 lines/mm grating, resulting in a 3 cm^{-1} resolution at 555 cm^{-1}. The samples, solution drops or solid, were placed on a clean gold-coated glass slide and exposed to the laser radiation for 60 s at ∼22 °C.

Magnesium chloride hexahydrate ($MgCl_2$•$6H_2O$; ACS certified) was obtained from Fisher Scientific (Pittsburgh, PA). Deionized water was obtained from a Barnstead Nanopure filtration system with a minimum resistivity of 18.2 MΩ•cm. A saturated aqueous solution of magnesium chloride was prepared and then filtered through a Whatman Carbon-Cap activated carbon filter to remove organic contaminants. The concentration of the filtered solution was determined by the Mohr method.[59] This solution was then diluted in deionized water to the final concentration in molarity. To prepare the two highest concentration solutions, the filtered solution was partially evaporated for several hours at 70 °C to the final concentrations. The $MgCl_2$ mole fraction concentrations used were 0.02x, 0.04x, 0.06x, and 0.09x. Mole fractions were calculated using densities from the literature.[60] Because our experimental temperature was lower than that reported by Phang et al., our mole fractions are overestimated and therefore reported to the second decimal. Concentrations of the $MgCl_2$ aqueous solutions expressed in molarity, mole fraction, and the calculated number of water molecules per $MgCl_2$ molecule are listed in Table 2.

TABLE 2: Concentrations of the $MgCl_2$ Aqueous Solutions Studied

molarity (mol/L)	mole fraction (x)	number of water molecules per $MgCl_2$
1.1	0.02	49
2.1	0.04	25
3.1	0.06	16
4.7	0.09	10
6.1	0.10	9

3. Results and Discussion

Early on in this study we observed that in the simulation started with magnesium chloride ion pairs present in the initial configuration, the water in the solvation shell of ion-paired magnesium was more mobile, and additional chloride ions were able to move in to form ion pairs with the magnesium. Approximately 95% of the magnesium dications were involved in contact ion-pairs in a 0.0888x bulk simulation. This does not seem unreasonable, as there are only ∼10 water molecules per $MgCl_2$ at this concentration. However, it is not necessarily correct. Alternatively, if no ion pairs were present in the initial configuration, then none formed during up to 6 ns of simulations for concentrations up to 0.100x. It seemed imperative, therefore, to determine first whether contact ion pairing should occur in $MgCl_2$ solutions, and second, whether a strong energetic argument can justify choosing initial conditions without contact ion pairs.

3.1. Potentials of Mean Force. The behavior of the simulated $MgCl_2$ solutions in the presence and absence of ion pairs in the initial conditions can be explained energetically with a PMF calculation in which the Helmholtz free energy required to move a chloride ion or water molecule toward magnesium is obtained as a function of distance from magnesium. In Figure 2 the results obtained with the Callahan force field for magne-

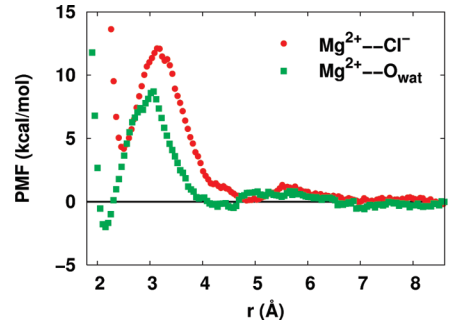

Figure 2. The potential of mean force (free energy) as a function of distance from the Mg^{2+} ion for $Mg^{2+}-Cl^-$ and $Mg^{2+}-O_{water}$ interactions in a solution at "infinite dilution" (0.0022x, 0.12 M).

sium are shown. The change in the free energy between a chloride outside the first solvation shell ($r > 4$ Å) and in a contact ion pair ($r \sim 2$ Å) is ~3.2 kcal/mol, whereas water in the first solvation shell of magnesium ($r \sim 2$ Å) is ~1.6 kcal/mol lower in energy than water in the second shell and beyond. This suggests that over long time scales, at equilibrium, magnesium will prefer a complete first solvation shell of water according to the Boltzmann distribution. However, there is a large barrier for either water or chloride to pass between the first and second solvation shells. The residence time for water in the first solvation shell of Mg^{2+} in our simulation is estimated using transition state theory to be 9.2 μs.[61] To obtain this estimate of the residence time, we have assumed that all waters (or chlorides) reaching the top of the barrier between solvation shells pass to the second shell, and therefore the pre-exponential factor is approximated as k_BT/h. While this overestimates the rate of escape, and underestimates the residence time, it is sufficient to establish the long residence time of constituents of the first solvation shell of magnesium. Our value for the residence time is larger than those reported in the simulation literature; however, frequently, these are reported as >5 ns or >10 ns, which is roughly in agreement with our findings.[45,62,63] These results are also in qualitative agreement with the results from ^{17}O NMR mentioned earlier, in which the lifetime of water in the first solvation shell of magnesium was reported to be >1.8 μs in 0.063*x* $Mg(ClO_4)_2$.[45] While not measured by the ^{17}O NMR experiment, the survival time of chloride in the first shell of Mg^{2+} is calculated from the PMF to be 84 ns. In any case, the main result is that, while current computer capabilities do not truly allow us to reach equilibrium when the initial conditions include contact ion pairs, PMF calculations suggest that it is reasonable to omit them from the initial conditions. Solvent-shared ion pairs ($r \sim 5$ Å) are energetically more favorable than contact ion pairs. In these pairs, magnesium and chloride are separated by one or more water molecules, which are in the first solvation shell of both ions. Additionally, the 1.38 ps survival time for solvent-shared ion pairs calculated from the PMF shows that, if we can assume that contact ion pairing does not occur, our classical MD simulations can easily sample the relevant structural features of aqueous $MgCl_2$ solutions at ambient temperatures.

The PMFs reported in Figure 2 explain the behavior observed in simulations with only one model. Comparison to calculations with other models and, ideally, comparison to experimental data is necessary to show definitively whether or not magnesium chloride forms contact ion pairs. Recently, in published simulations based on nonpolarizable force field descriptions of magnesium chloride, Larentzos and Criscenti have also shown contact ion pairs between magnesium and chloride to be disfavored.[63] In addition, a similar PMF study of magnesium nitrate again showed the absence of ion pairing, and that study was substantiated by a Raman spectroscopic study of the bond between Mg^{2+} and the oxygen atoms of water in its first solvation shell.[64] We next report a similar, concentration-dependent Raman spectroscopic study for the $Mg^{2+}-O_{water}$ stretch in solutions of magnesium chloride.

3.2. Raman Spectroscopy of the $Mg^{2+}-O_{water}$ Stretch. Raman spectra of aqueous $MgCl_2$ solutions of 0.02*x*, 0.04*x*, 0.06*x*, and 0.09*x* were acquired in the $Mg^{2+}-O_{water}$ stretching region as shown in Figure 3a. A neat water spectrum is included for comparison. The intermolecular $Mg^{2+}-O_{water}$ peak is observed at ~355 cm^{-1}. This peak has been referred to as the hexaaquo $Mg(H_2O)_6^{2+}$ stretch.[41,65,66] The peak area obtained by curve-fitting increases with increasing concentration as shown

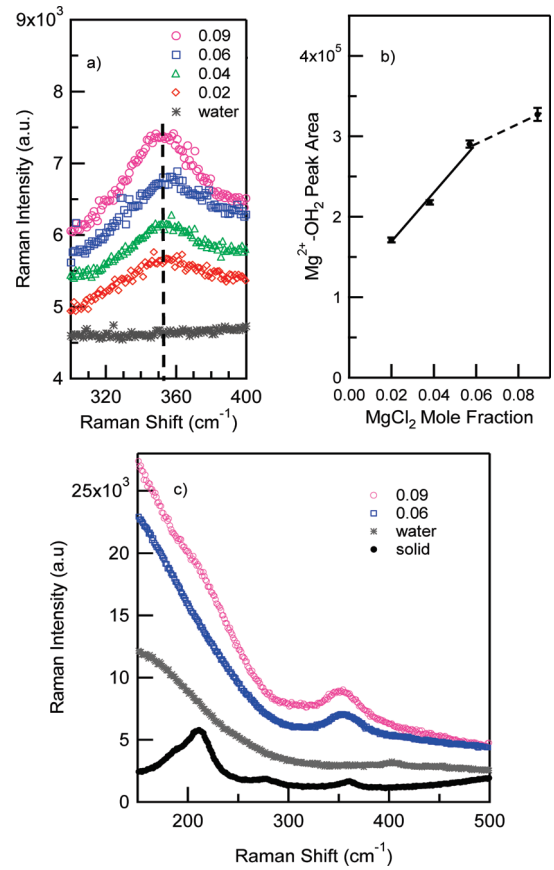

Figure 3. (a) Raman spectra of the ($Mg^{2+}-O_{water}$) stretching vibration for aqueous solutions of $MgCl_2$ at different mole fraction concentrations. (b) The area under the ($Mg^{2+}-O_{water}$) peak as a function of $MgCl_2$ concentration. (c) Lower frequency Raman spectra of 0.09*x* $MgCl_2$ solution and the solid $MgCl_2 \cdot 6H_2O$ reveal a broad band from 190 to 230 cm^{-1} that is not evident in the spectra from 0.06*x* solution and neat water. In plots a and c, spectra are shown with an adjusted *y* axis for ease of viewing, and neat water spectra are included for reference.

in Figure 3b. The analysis reveals a linear correlation between the peak area of the $Mg^{2+}-O_{water}$ band and concentration up to the 0.06*x* $MgCl_2$ aqueous solution. This linearity suggests that Mg^{2+} cation maintains the six water molecules in its first hydration shell. At 0.09*x* $MgCl_2$ there is a deviation from linear behavior suggesting a different solvation environment for Mg^{2+} where the primary solvation shell of Mg^{2+} is perturbed, likely due to the fewer number of water molecules available per $MgCl_2$ (Table 2; 10 water molecules per $MgCl_2$). In addition, the Raman spectrum of the 0.09*x* aqueous solution reveals a 6 cm^{-1} red shift, 354 cm^{-1} to 348 cm^{-1}, consistent with a perturbed Mg^{2+} hydration environment. While this shift is attributed to a change in hydration environment, it is not assigned to the formation of contact ion pairs. To further evaluate the 0.09*x* solution and to confirm lack of contact ion pairing, we obtained additional Raman spectra lower in frequency and compared the spectra from the 0.09*x* and 0.06*x* solutions to that of the solid $MgCl_2 \cdot 6H_2O$ as shown in Figure 3c. We observe a broadband from 190 to 250 cm^{-1} in the 0.09*x* solution spectrum, which is not evident in the 0.06*x* spectrum, nor in the neat water spectrum. Although from previous work the appearance of a peak at ~240 cm^{-1} and 230 cm^{-1} was attributed to $Mg^{2+}-Cl^-$ contact ion pairs from melts,[67−69] from aqueous mixtures of Na^+, Mg^{2+}, Cl^-, and SO_4^{2-} at 25 °C,[70] and from $MgCl_2$ thin films,[71] we observe resonances in this spectral region from the solid $MgCl_2 \cdot 6H_2O$ as shown in Figure 3c. These bands from the solid

sample arise from the fully hydrated Mg^{2+} ion without contact ion pairing between Mg^{2+} and Cl^- ions and are attributed to a phonon band arising from some long-range order[15] in the high concentration solution and are observed here in a fully hydrated Mg^{2+} scenario. The crystalline structure of $MgCl_2 \cdot 6H_2O$ has been confirmed using X-ray diffraction.[72] The observed resonance centered at $\sim$230 cm^{-1} and the observed frequency shift of the 355 cm^{-1} peak from the 0.09*x* $MgCl_2$ solution are therefore consistent with a perturbed hydration environment of fully hydrated Mg^{2+} ions in the 0.09*x* solution. Hence, there is no clear spectral evidence that contact ion pairing occurs in the solutions studied here, even for the high concentration solution of 0.09*x* (4.7 M) $MgCl_2$.

By analyzing the number of water molecules available for solvation at each concentration studied here, and recognizing that Mg^{2+} is more efficient at attracting hydration water relative to Cl^-, we find that, in the lower concentration solutions (0.02*x*, 0.04*x*, and 0.06*x*), it is likely that a large portion of the ions have a complete first and even the second solvation shell. For the 0.09*x* $MgCl_2$ solution, there are insufficient numbers of water molecules available to fill the second solvation shell of Mg^{2+}, or to complete the first solvation shell of all the ions; therefore, substantial solvent-shared ion pairing is unavoidable. A change in the hydration environment of Mg^{2+} at the highest concentration can be easily envisioned when considering that at 0.06*x* there are 10 water molecules in addition to the six water molecules of the first solvation shell for each Mg^{2+}. According to previous research, the remaining 10 (0.06*x*) water molecules are sufficient to complete a second hydration shell around Mg^{2+} and/or to solvate the Cl^- ions.[41,73,74] However, some solvent-shared ion pairs are still expected, even at low concentrations, since the PMF calculated earlier in the paper shows no energetic preference between solvent-shared and solvent-separated ion pairs in this system. The portion of ions in solvent-shared ion pairs is expected to increase with concentration. Additionally, as concentration increases, some chloride ions will form solvent-shared ion pairs with more than one hydrated magnesium ion simultaneously. At 0.09*x* there are only four water molecules in addition to the first solvation shell for each Mg^{2+} ion. Therefore, there are a large number of solvent-shared ion pairs at this higher concentration.

3.3. Comparison of MD and Experimental Densities. At concentrations around 0.09*x* there are changes in the Raman spectrum of the $Mg^{2+}-O_{water}$ region that are indicative of a change in the solution structure at high concentration, although they do not suggest contact ion pairing between Mg^{2+} and Cl^-. Previous studies of osmotic potential have also concluded that there is an absence of contact ion pairing in $MgCl_2$ solutions even at saturation,[75,76] although studies of the speed of sound in solution,[77] viscosity,[78] and apparent molal volumes[79] suggest that a structural change, which is not necessarily the onset ion pairing, does occur near 4*m* (0.07*x*) in aqueous $MgCl_2$. Therefore we provide a comparison of simulation results for $MgCl_2$ solutions with and without contact ion pairs to additional experimental data. The information compared will be used to solidify the evidence suggesting the absence of ion pairing in $MgCl_2$ solutions and to provide insight into the structure of these solutions. The bulk densities of 0.0888*x* (4.45 M) $MgCl_2$ solutions obtained with each of the Mg^{2+} parameter sets in the presence and absence of ion pairs are presented in Table 3. The absence of ion pairing in simulations greatly improves the densities of the concentrated solutions for all of the Mg^{2+} parameter sets employed in this study.[80]

TABLE 3: Density Data for Concentrated Bulk Solutions from Experiment and from MD Simulations with and without Contact Ion Pairing in the Initial Configuration

0.0888*x* $MgCl_2$	with ion pairs		without ion pairs	
Mg^{2+} parameter set	bulk density (g/mL)	% error	bulk density (g/mL)	% error
experiment[80]	1.295		1.295	
Åqvist/ff99	1.162 ± 0.005	10.27	1.3077 ± 0.005	0.981
OPLSAA	1.198 ± 0.008	7.49	1.2799 ± 0.005	1.17
Callahan	1.210 ± 0.004	6.56	1.2458 ± 0.004	3.80

3.4. Comparison of MD and Diffraction Experiments. An atomistic measure of liquid structure can be derived from X-ray and neutron diffraction data. Historically, X-ray diffraction suggested that magnesium chloride does not form ion pairs.[20,81−83] Here we directly compare a total radial distribution function (RDF) obtained from X-ray diffraction of 0.0802*x* $MgCl_2$ by Caminiti et al.[82] with those calculated from MD simulations of magnesium chloride, with and without ion pairing, using the ff99, OPLSAA, and Callahan force fields for magnesium. RDFs were computed for each pair of atoms in the 0.0888*x* bulk $MgCl_2$ systems, and the pair RDFs were weighted by the concentrations and atomic form factors[84,85] and summed for direct comparison to the total RDFs derived from X-ray diffraction experiments.[86,87]

Figure 4 displays the weighted total RDFs as red lines denoted "Simulated $g(r)$," for 0.0888*x* solutions of $MgCl_2$ for each of three Mg^{2+} parameter sets. Each plot includes a direct comparison with the RDF obtained using X-ray diffraction by Caminiti et al. (black crosses).[82] Additionally, the contributions of each weighted pair RDF are shown. At first glance, the agreement between total RDFs calculated from MD simulations and the experimental RDF improves greatly in the absence of ion pairing.

There are three main features in the total RDF from X-ray diffraction:

The peak around 2.1 Å is attributed to water in the first solvation shell of magnesium dication.[82] A survey of X-ray diffraction data in the literature give a range of 2.0 Å to 2.12 Å as the $Mg^{2+}-O_{water}$ distance.[20,81−83,88,89] In the computed RDFs from solutions with ion pairs (left column of Figure 4), we note that there is an additional contribution from chloride−magnesium contact ion pairs. We find that the $Mg^{2+}-O_{water}$ distance in ff99 with ion pairs is $\sim$0.2 Å shorter than in experiment (green peak, bottom left of Figure 4).

The peak in the RDF around 3 Å comes from $O_{water}-O_{water}$ (blue) and Cl^-O_{water} (gold) interactions. Additionally, in the $g(r)$ from simulations with contact ion pairs, contributions from chloride−magnesium ion pairs contribute to a shoulder at 2.5 Å (cyan, left column of Figure 3). It is worth noting that the effects of slight differences in the Mg^{2+} parameters affect $O_{water}-O_{water}$ RDFs, even in systems where the absence of ion pairing means each magnesium is completely surrounded by a shell of water. We note that agreement with experiment is better in the absence of ion pairing, and that the Callahan Mg^{2+} force field results in the best agreement in this region.

Around 4.5 Å there are peaks due to correlations of pairs that are separated by a water or ion, such as correlations from second solvation shells. The best agreement with experimental values for this peak and the minimum before it ($r \sim 3.5$ Å) is found in the absence of ion pairing. After these peaks and the depression that follows it, the structure is less noticeable.

From the RDF's and the corresponding coordination numbers, we can develop a concrete picture of the solvation environment of magnesium at 0.0888*x*. First, six water molecules are

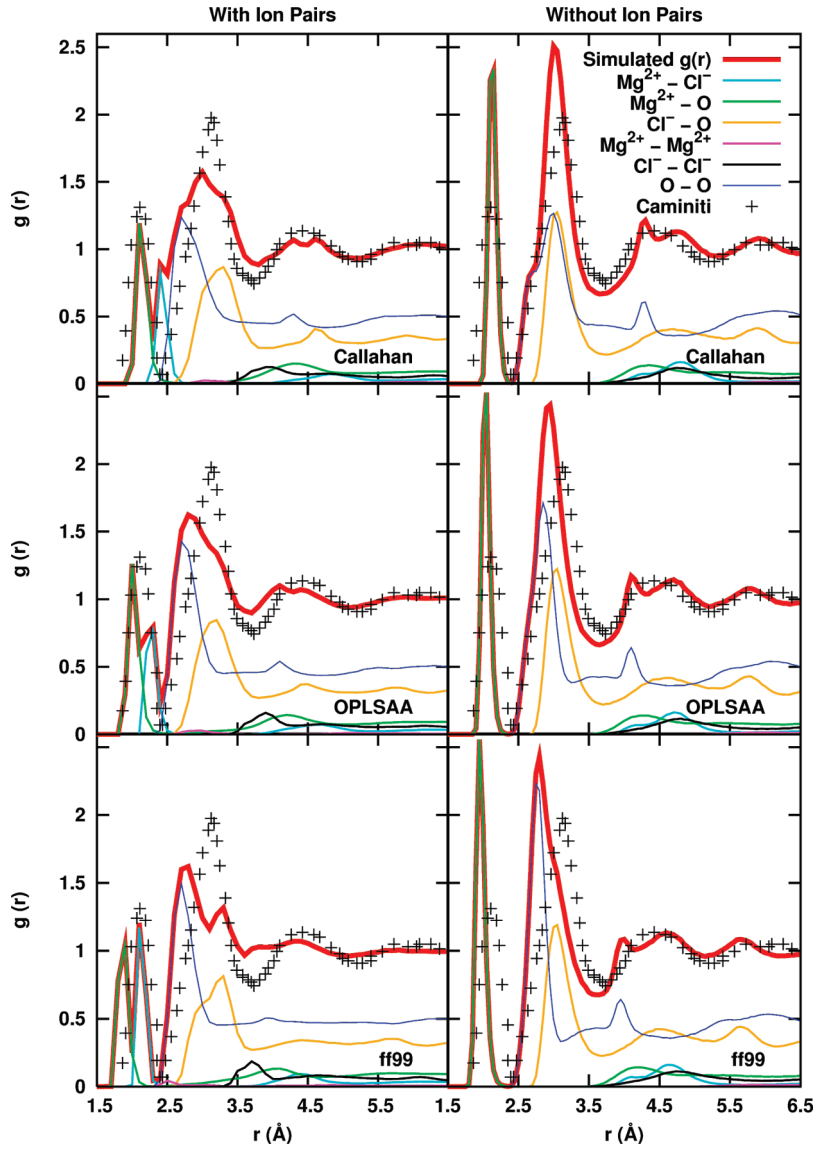

Figure 4. Total RDFs and pair contributions from 0.0888*x* $MgCl_2$ simulations using the Mg^{2+} parameters denoted in the bottom right corner of each plot, compared to the total RDF derived from an X-ray diffraction experiment by Caminiti et al. of 0.0802*x* $MgCl_2$.[82]

coordinated to each magnesium cation in a tight octahedral pattern. There are approximately six additional waters per magnesium that contribute to the second solvation shell of magnesium and solvation of chloride. There are no contact ion pairs between chloride and magnesium. Chloride anions coordinate 3.2 hydrated magnesium cations on average, within a cutoff distance of 5.9 Å for solvent-shared ion pairs. Each hydrated magnesium cation coordinates with 6.4 chloride anions on average. In addition, the first solvation shells of Mg^{2+} will have some contact with each other. Therefore, we expect the environment of solvated magnesium in these high concentration $MgCl_2$ solutions to be greatly perturbed compared to solutions of lower concentrations.

We have established that Raman spectra of the $Mg^{2+}-O_{water}$ stretch show that contact ion pairing is very unlikely below 0.06*x* and not observed even at 0.09*x*, although noticeable changes to the environment of these bonds affect the spectra of $MgCl_2$ solutions at 0.09*x*. Additionally, both bulk density and RDFs at high concentration are in better agreement with experimental data when ion pairing is avoided. We firmly conclude that contact ion pairing is not observed in aqueous solutions of $MgCl_2$ up to fairly high concentrations, and it is therefore reasonable to perform simulations with magnesium that do not include contact ion pairing. Additionally, for simulations with the PB Cl^- and the POL3 water models, we find that the Mg^{2+} model developed here, as well as the OPLS model, give good agreement with the total RDF from X-ray diffraction.

It is worth noting that magnesium can and does form contact ion pairs in other solvents, in enzymes, and with some other counterions. For example, Raman studies by Pye and Rudolph suggest that Mg^{2+} can contact ion pair with sulfate.[41] Similarly, ultrasonic absorption has been used by Fisher to determine the concentration of magnesium sulfate ion pairs in seawater.[90] Studies by Wahib et al. and Minofar et al. have also shown that Mg^{2+} may contact ion pair with acetate.[91,92] Individual phosphate groups on the backbone of RNA can bind directly to Mg^{2+}, replacing one or two water molecules in the hexahydrate structure.[4] Whether classical equilibrium MD of systems containing magnesium dications is feasible has to be determined on a case by case basis.

There is one further caveat that we wish to express concerning X-ray and neutron diffraction difference methods that have been used to obtain more detailed structural data on $MgCl_2$. Mg^{2+} isotopes do not have sufficiently different scattering cross

sections for neutron difference spectra to be useful.[89] It is known from extensive studies with X-ray diffraction and extended X-ray absorption fine structure (EXAFS) that Ni^{2+} coordinates approximately the same number of water molecules at approximately the same distance as Mg^{2+}.[89,93−99] Ni^{2+} scatters X-rays more strongly than Mg^{2+}.[89,93−99] On the basis of these properties, X-ray difference spectra have been obtained using Ni^{2+} as a structural isomorph to Mg^{2+}.[89] However, at 1 M $NiCl_2$, about 14−22% of Ni^{2+} are observed to be paired with Cl^-.[100,101] At 3−4 M it is observed that 30−60% of Ni^{2+} is ion paired, and some Ni^{2+} may coordinate more than one Cl^-.[94,96,102] Therefore, we would urge caution in considering $MgCl_2$ and $NiCl_2$ to be structurally analogous, in light of the apparently large difference in the ion pairing propensities of Mg^{2+} and Ni^{2+}.

4. Conclusions

We have shown, on the basis of comparison of MD simulation to the X-ray diffraction work of Caminiti et al.[82] and Raman spectra of the $Mg^{2+}-O_{water}$ stretch obtained in this study, that it is unlikely that aqueous $MgCl_2$ forms contact ion pairs at ambient pressure and temperature even at concentrations approaching saturation. Additionally, based on PMF calculations with our newly developed force field, we have shown that contact ion pairs are energetically unfavorable for magnesium chloride, and that it is reasonable to avoid $Mg^{2+}-Cl^-$ contact ion pairs in the initial conditions of the simulation runs. This makes it possible to sample relevant states in the simulations rather than remain trapped behind large energy barriers. The strong hydration, lack of contact ion pairing to chloride, and ability to strongly orient water, as predicted by simulations and observed through vibrational spectroscopic techniques, makes magnesium dication possibly unique among cations in its effects on the solution environment.

Acknowledgment. K.M.C. is grateful for a fellowship from the Department of Education Graduate Assistance in Areas of National Need (GAANN) program. K.M.C. and D.J.T. acknowledge support from the National Science Foundation (Grants CHE-0431512 and CHE-0909227). N.N.C.I. and H.C.A. acknowledge support from the U.S. Department of Energy Office of Basic Energy Sciences, Division of Chemical Sciences, Geosciences (DOE-BES, DE-FG02-04ER15495). M.R. acknowledges the support of the Ministry of Education of the Czech Republic (Grants ME09064 and LC512). Part of the work in Prague was supported via Project Z40550506.

References and Notes

(1) Cowan, J. A. *Biometals* **2002**, *15*, 225.
(2) Jiao, D.; King, C.; Grossfield, A.; Darden, T. A.; Ren, P. *J. Phys. Chem. B* **2006**, *110*, 18553.
(3) Bernasconi, L.; Baerends, E. J.; Sprik, M. *J. Phys. Chem. B* **2006**, *110*, 11444.
(4) Gong, B.; Chen, Y.; Christian, E. L.; Chen, J.-H.; Chase, E.; Chadalavada, D. M.; Yajima, R.; Golden, B. L.; Bevilacqua, P. C.; Carey, P. R. *J. Am. Chem. Soc.* **2008**, *130*, 9670.
(5) *CRC Handbook of Chemistry and Physics*, 77th ed.; CRC Press: Boca Raton, FL, 1996.
(6) Greenspan, L. *J. Res. Natl. Bur. Stand.* **1977**, *81A*, 89.
(7) Shaka', H.; Robertson, W. H.; Finlayson-Pitts, B. J. *Phys. Chem. Chem. Phys.* **2007**, *9*, 1980.
(8) Finlayson-Pitts, B. J. *Chem. Rev.* **2003**, *103*, 4801.
(9) Knipping, E. M.; Lakin, M. J.; Foster, K. L.; Jungwirth, P.; Tobias, D. J.; Gerber, R. B.; Dabdub, D.; Finlayson-Pitts, B. J. *Science* **2000**, *288*, 301.
(10) Gill, T. E.; Gillette, D. A.; Niemeyer, T.; Winn, R. T. *Nucl. Instrum. Methods B* **2002**, *189*, 209.
(11) Gill, T. E.; Gillette, D. A. *Geol. Soc. Am. Abstr. Programs* **1991**, *23*, 462.
(12) Choi, M. Y.; Chan, C. K. *J. Chem. Eng. Data* **2002**, *47*, 1526.
(13) Gibson, E. R.; Hudson, P. K.; Grassian, V. H. *J. Phys. Chem. A* **2006**, *110*, 11785.
(14) Callahan, K. M.; Casillas-Ituarte, N. N.; Xu, M.; Roeselová, M.; Allen, H. C.; Tobias, D. J. *J. Phys. Chem. A*, submitted for publication, 2009.
(15) Casillas-Ituarte, N. N.; Callahan, K. M.; Tang, C. Y.; Chen, X.; Roeselová, M.; Tobias, D. J.; Allen, H. C. *Proc. Natl. Acad. Sci. U.S.A.*, in press, 2010.
(16) Dietz, W.; Riede, W. O.; Heinzinger, K. *Z. Naturforsch.* **1982**, *37a*, 1038.
(17) Bock, C.; Markham, G.; Katz, A.; Glusker, J. *Theor. Chem. Acc.* **2006**, *115*, 100.
(18) Guàrdia, E.; Sesé, G.; Padró, J. A.; Kalko, S. G. *J. Solution Chem.* **1999**, *28*, 1113.
(19) Szász, G. I.; Dietz, W.; Heinzinger, K.; Pálinkás, G.; Radnai, T. *Chem. Phys. Lett.* **1982**, *92*, 388.
(20) Pálinkás, G.; Radnai, T.; Dietz, W.; Szász, G. I.; Heinzinger, K. *Z. Naturforsch.* **1982**, *37a*, 1049.
(21) Heinzinger, K. *Physica* **1985**, *131B*, 196.
(22) Zapalowski, M.; Bartczak, W. M. *Res. Chem. Intermed.* **2001**, *27*, 855.
(23) Lightstone, F. C.; Schwegler, E.; Hood, R. Q.; Gygi, F.; Galli, G. *Chem. Phys. Lett.* **2001**, *343*, 549.
(24) Krekeler, C.; Delle Site, L. *J. Phys.: Condens. Matter* **2007**, *19*, 192101.
(25) Tongraar, A.; Rode, B. M. *Chem. Phys. Lett.* **2005**, *409*, 304.
(26) Tongraar, A.; Rode, B. M. *Chem. Phys. Lett.* **2001**, *346*, 485.
(27) Ikeda, T.; Boero, M.; Terakura, K. *J. Chem. Phys.* **2007**, *127*, 074503.
(28) Tofteberg, T.; Öhrn, A.; Karlström, G. *Chem. Phys. Lett.* **2006**, *429*, 436.
(29) Markham, G. D.; Glusker, J. P.; Bock, C. L.; Trachtman, M.; Bock, C. W. *J. Phys. Chem.* **1996**, *100*, 3488.
(30) Markham, G.; Glusker, J.; Bock, C. *J. Phys. Chem. B* **2002**, *106*, 5118.
(31) Jagoda-Cwiklik, B.; Jungwirth, P.; Rulísek, L.; Milko, P.; Roithová, J.; Lemaire, J.; Maitre, P.; Ortega, J. M.; Schröder, D. *ChemPhysChem* **2007**, *8*, 1629.
(32) Bock, C.; Markham, G.; Katz, A.; Glusker, J. *Theor. Chem. Acc.* **2006**, *115*, 100.
(33) Bock, C.; Kaufman, A.; Glusker, J. *Inorg. Chem.* **1994**, *33*, 419.
(34) Spångberg, D.; Hermansson, K. *J. Chem. Phys.* **2003**, *119*, 7263.
(35) Adrian-Scotto, M.; Mallet, G.; Vasilescu, D. *J. Mol. Struct.* **2005**, *728*, 231.
(36) Waizumi, K.; Masuda, I.; Fukushima, N. *Chem. Phys. Lett.* **1993**, *205*, 317.
(37) Martínez, J. M.; Pappalardo, R. R.; Marcos, E. S. *J. Am. Chem. Soc.* **1999**, *121*, 3175.
(38) Pavlov, M.; Siegbahn, P. E.; Sandström, M. *J. Phys. Chem. A* **1998**, *102*, 219.
(39) Krekeler, C.; Delle Site, L. *J. Chem. Phys.* **2008**, *128*, 134515.
(40) Struis, R. P. W. J.; De Bleijser, J.; Leyte, J. C. *J. Phys. Chem.* **1989**, *93*, 7943.
(41) Pye, C. C.; Rudolph, W. W. *J. Phys. Chem. A* **1998**, *102*, 9933.
(42) Cappa, C. D.; Smith, J. D.; Messer, B. M.; Cohen, R. C.; Saykally, R. J. *J. Phys. Chem. B* **2006**, *110*, 5301.
(43) Xu, M.; Larentzos, J. P.; Roshdy, M.; Criscenti, L. J.; Allen, H. C. *Phys. Chem. Chem. Phys.* **2008**, *10*, 4793.
(44) Xu, M.; Tang, C. Y.; Jubb, A. M.; Chen, X.; Allen, H. C. *J. Phys. Chem. C* **2009**, *113*, 2082.
(45) Neely, J.; Connick, R. *J. Am. Chem. Soc.* **1970**, *92*, 3476.
(46) Grossfield, A. *Weighted Histogram Analysis Method*, 2.0.2 ed.; University of Rochester Medical Center: Rochester, NY, 2008.
(47) Cornell, W. D.; Cieplak, P.; Bayly, C. I.; Gould, I. R.; Merz, K. M.; Ferguson, D. M.; Spellmeyer, D. C.; Fox, T.; Caldwell, J. W.; Kollman, P. A. *J. Am. Chem. Soc.* **1995**, *117*, 5179.
(48) Case, D. A.; Darden, T. A.; Cheatham, T. E., III; Simmerling, C. L.; Wang, J.; Duke, R. E.; Luo, R.; Merz, K. M.; Wang, B.; Pearlman, D. A.; Crowley, M.; Brozell, S.; Tsui, V.; Gohlke, H.; Mongan, J.; Hornak, V.; Cui, G.; Beroza, P.; Schafmeister, C.; Caldwell, J. W.; Ross, W. S.; Kollman, P. A. *AMBER 8*; University of California: San Francisco, 2004.
(49) Åqvist, J. *J. Phys. Chem.* **1990**, *94*, 8021.
(50) Jorgensen, W. L. *Parameters for Organic Molecules, Ions, and Nucleic Acids*; Yale University: New Haven, CT, 1997.
(51) Caldwell, J. W.; Kollman, P. A. *J. Phys. Chem.* **1995**, *99*, 6208.
(52) Perera, L.; Berkowitz, M. L. *J. Chem. Phys.* **1991**, *95*, 1954.
(53) Petersen, P. B.; Saykally, R. J.; Mucha, M.; Jungwirth, P. *J. Phys. Chem. B* **2005**, *109*, 10915.
(54) Essmann, U.; Perera, L.; Berkowitz, M. L.; Darden, T.; Lee, H.; Pedersen, L. G. *J. Chem. Phys.* **1995**, *103*, 8577.
(55) Darden, T.; York, D.; Pedersen, L. *J. Chem. Phys.* **1993**, *98*, 10089.
(56) Ryckaert, J. P.; Ciccotti, G.; Berendsen, H. J. C. *J. Comp. Phys.* **1977**, *23*, 327.

(57) Berendsen, H. J. C.; Postma, J. P. M.; van Gunsteren, W. F.; DiNola, A.; Haak, J. R. *J. Chem. Phys.* **1984**, *81*, 3684.
(58) Humphrey, W.; Dalke, A.; Schulten, K. *J. Mol. Graphics* **1996**, *14*, 33.
(59) Doughty, H. W. *J. Am. Chem. Soc.* **1924**, *46*, 2707.
(60) Phang, S.; Stokes, R. H. *J. Solution Chem.* **1980**, *9*, 497.
(61) Zwanzig, R. *Nonequilibrium Statistical Mechanics*, 5th ed.; Oxford University Press: New York, 2001.
(62) Bleuzen, A.; Pittet, P.-A.; Helm, L.; Merbach, A. E. *Magn. Reson. Chem.* **1997**, *35*, 765.
(63) Larentzos, J. P.; Criscenti, L. J. *J. Phys. Chem. B* **2008**, *112*, 14243.
(64) Xu, M.; Larentzos, J.; Roshdy, M.; Criscenti, L. J.; Allen, H. C. *Phys. Chem. Chem. Phys.* **2008**, *10*, 4793.
(65) Mink, J.; Németh, C.; Hajba, L.; Sandström, D. R.; Goggin, P. L. *J. Mol. Struct.* **2003**, *661*−*662*, 141.
(66) Rudolph, W. W.; Irmer, G.; Hefter, G. T. *Phys. Chem. Chem. Phys.* **2003**, *5*, 5253.
(67) *Thermodynamic Properties of Complex Fluid Mixtures*; Wiley-VCH: Weinheim, Germany, 2004.
(68) Capwell, R. J. *Chem. Phys. Lett.* **1972**, *12*, 443.
(69) Huang, C.-H.; Brooker, M. H. *Chem. Phys. Lett.* **1976**, *43*, 180.
(70) Tepavitcharova, S.; Balarew, C.; Rull, F.; Rabadjieva, D.; Iliev, A. *J. Raman Spectrosc.* **2005**, *36*, 891.
(71) Sano, H.; Miyaoka, H.; T., K.; H., M.; G, M.; N., O.; M., T. *Surf. Sci.* **2002**, *502*−*503*, 70.
(72) Sugimoto, K.; Dinnebier, R. E.; Hanson, J. C. *Acta Crystallogr., Sect. B* **2007**, *63*, 235.
(73) Smirnov, P. R.; Trostin, V. N. *Russ. J. Gen. Chem.* **2008**, *78*, 1643.
(74) Bernal-Uruchurtu, M. I.; Ortega-Blake, I. *J. Chem. Phys.* **1995**, *103*, 1588.
(75) Miladinović, J.; Ninković, R.; Todorović, M. *J. Solution Chem.* **2007**, *36*, 1401.
(76) Phutela, R. C.; Pitzer, K. S. *J. Solution Chem.* **1983**, *12*, 201.
(77) Millero, F. J.; Fernandez, M.; Vinokurova, F. *J. Phys. Chem.* **1985**, *89*, 1062.
(78) Mahluddin, S.; Ismail, K. *J. Phys. Chem.* **1983**, *87*, 5241.
(79) Monnin, C. *J. Solution Chem.* **1987**, *16*, 1035.
(80) Söhnel, O.; Novotny, P. *Densities of Aqueous Solutions of Inorganic Substances*; Elsevier Science Publishing Co.: Amsterdam, 1985.
(81) Dorosh, A. K.; Skryshevskii, A. F. *Zh. Strukt. Khim.* **1964**, *5*, 911.
(82) Caminiti, R.; Licheri, G.; Piccaluga, G.; Pinna, G. *J. Appl. Crystallogr.* **1979**, *12*, 34.
(83) Caminiti, R.; Licheri, G.; Piccaluga, G.; Pinna, G. *Chem. Phys. Lett.* **1977**, *47*, 275.
(84) Cromer, D. T.; Mann, J. B. *Acta Crystallogr. A* **1968**, *24*, 321.
(85) Hadju, F. *Acta Crystallogr. A* **1972**, *28*, 250.
(86) Mason, P. E.; Neilson, G. W.; Kline, S. R.; Dempsey, C. E.; Brady, J. W. *J. Phys. Chem. B* **2006**, *110*, 13477.
(87) Mason, P. E.; Ansell, S.; Neilson, G. W. *J. Phys.: Condens. Matter* **2006**, *18*, 8437.
(88) Albright, J. N. *J. Chem. Phys.* **1972**, *56*, 3783.
(89) Skipper, N. T.; Neilson, G. W.; Cummings, S. C. *J. Phys.: Condens. Matter* **1989**, *1*, 3489.
(90) Fisher, F. H. *Science* **1967**, *157*, 823.
(91) Wahab, A.; Mahiuddin, S.; Hefter, G.; Kunz, W.; Minofar, B.; Jungwirth, P. *J. Phys. Chem. B* **2005**, *109*, 24108.
(92) Minofar, B.; Vácha, R.; Wahab, A.; Mahiuddin, S.; Kunz, W.; Jungwirth, P. *J. Phys. Chem. B* **2006**, *110*, 15939.
(93) Magini, M. *J. Chem. Phys.* **1981**, *74*, 2523.
(94) Magini, M.; Paschina, G.; Piccaluga, G. *J. Chem. Phys.* **1982**, *76*, 1116.
(95) Neilson, G. W.; Enderby, J. E. *Proc. R. Soc. A* **1983**, *390*, 353.
(96) Licheri, G.; Paschina, G.; Piccaluga, G.; Pinna, G.; Vlaic, G. *Chem. Phys. Lett.* **1981**, *83*, 384.
(97) Licheri, G.; Paschina, G.; Piccaluga, G.; Pinna, G. *J. Chem. Phys.* **1983**, *79*, 2168.
(98) Sandstrom, D. R. *J. Chem. Phys.* **1979**, *71*, 2381.
(99) Neilson, G. W.; Enderby, J. E. *J. Phys. C: Solid State Phys.* **1978**, *11*, L625.
(100) Weingarter, H.; Hertz, H. G. *J. Chem. Soc., Faraday Trans. 1* **1979**, *75*, 2700.
(101) Weingarter, H.; Müller, C.; Hertz, H. G. *J. Chem. Soc., Faraday Trans. 1* **1979**, *75*, 2712.
(102) Magini, M.; de Moraes, M.; Licheri, G.; Piccaluga, G. *J. Chem. Phys.* **1985**, *83*, 5797.

JP909132A